Predicting filament drift in twisted anisotropy

Marcel Wellner,[1,2] Omer Berenfeld,[1] and Arkady M. Pertsov[1]
[1]*Department of Pharmacology, SUNY Health Science Center at Syracuse, Syracuse, New York 132102*
[2]*Physics Department, Syracuse University, Syracuse, New York 13244*
(Received 25 August 1999)

Excitable media with twisted anisotropy have recently been attracting significant interest because of their applicability to wave propagation in heart tissue. Here we consider the dynamics of an intramural scroll wave whose filament lies initially within an arbitrary layer of mutually parallel cardiac fibers, and drifts parallel to itself from layer to layer. Earlier simulations have demonstrated that such a filament stabilizes in a layer whose fiber direction is the same as its own. In the present paper we analytically derive the trajectory of the filament, and obtain good agreement with earlier numerical data. For sufficiently sparse scrolls, our analysis predicts an equilibrium alignment perpendicular rather than parallel to the fibers.

PACS number(s): 82.40.Ck

I. INTRODUCTION

The heart muscle is a prime example of an excitable medium with nontrivial geometrical structure. To understand its wave activity it has been natural to ignore the geometry at first; but the next challenge to theoretical understanding has been to incorporate one of the principal features of that geometry, namely, twisted anisotropy [1,2]. Here we examine its effect on scroll waves, which are known to occur in heart tissue [3,4] and are a suspected cause of cardiac arrhythmias.

In the mammalian heart, sketched in Fig. 1, the anisotropy is manifested by a location-dependent direction of the muscle fibers, further complicated by the existence of curved layers of muscle interspersed with connective tissue. The fiber direction, or longitudinal direction, is associated with a greater speed of propagation for the excitation waves than the transverse directions. We focus our attention on an intramural scroll wave whose instantaneous filament resides within a layer of mutually parallel fibers, as indicated by the insets of Fig. 1. (We do not address the transmural case [5,6], nor do we address the effects of discreteness in the space lattice or in the actual tissue [7].)

In a recently published study [8], some of us have reported on the drifting behavior of such an intramural scroll wave whose end effects can be neglected. Initially, the filament intersects the fibers in its layer at an arbitrary angle; it is then found to drift parallel to itself towards an equilibrium layer where fibers and filament have the same direction. This scenario was obtained computationally, using a FitzHugh-Nagumo (FHN) model whose parameters were adjusted to produce physiologically reasonable wave forms. The present work concentrates on this process of parallel drift, and treats the phenomenon analytically; the result is a theoretical formula that predicts the drift velocity. Changes in the sign of the velocity are used to locate the equilibrium layers, and the direction of the change determines whether the equilibrium is stable or unstable. Integrating the velocity leads to a good prediction of the filament's trajectory in space time.

II. MEDIUM

In order to represent a limited sample of the cardiac wall it is instructive to model the twisted anisotropy in very simple geometrical terms as follows (cf. Ref. [8], with some minor differences in notation): Consider a z axis across the wall, and assume that each xy plane is uniformly anisotropic, with principal velocities of propagation $\mathbf{V}_{\max}$ and $\mathbf{V}_{\min}$ along the plane; their magnitudes $V_{\max}$ and $V_{\min}$ are independent of z. As z increases, the direction of anisotropy twists at a constant rate so that $\mathbf{V}_{\max}$ makes an angle

$$\theta = kz \tag{1}$$

with the x axis ($k=$ constant). We note that at $z=0$ the fibers are in the x direction, while at $z=\pi/2k$ they are in the y direction. In actual heart tissue, θ can change (albeit nonuni-

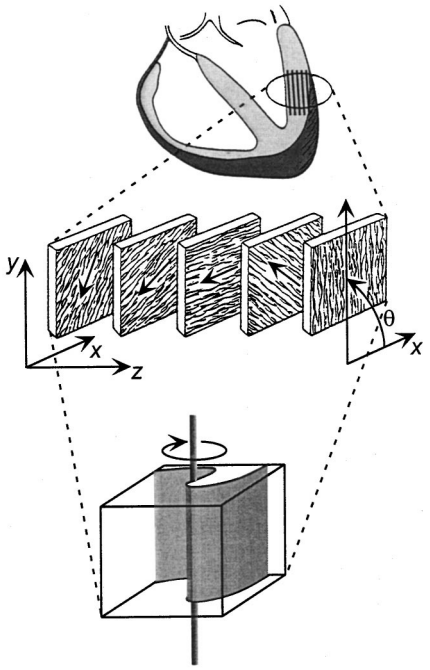

FIG. 1. Twisted anisotropy in the ventricular wall. In this sample location (top inset) the fibers rotate over about 120° across the wall. The dissected slices make up a cube, illustrated in the bottom inset. In the cube we show a snapshot of the scroll wave with its filament F. The latter can be thought of as lying within one of the tissue sections.

formly) by about 120° over the thickness of the ventricular free wall; as we have indicated above, the maximum velocity is in the direction of the muscular fibers. Propagation in the z direction will be considered to occur at speed $V_{\min}$.

Let the variables u and v propagate in a three-dimensional FHN-type medium according to

$$\partial_t u - \partial_i (D_{ij} \partial_j u) + \Phi_1(u,v) = 0, \tag{2}$$

$$\partial_t v + \Phi_2(u,v) = 0, \tag{3}$$

where Φ_1 and Φ_2 are generic reaction functions; in our notation we have $\{x_i\} = \{x,y,z\}$, and sums over repeated indices are understood. The diffusivity tensor has the components [8]

$$\begin{aligned} D_{11} &= D_L \cos^2\theta + D_T \sin^2\theta, \\ D_{22} &= D_L \sin^2\theta + D_T \cos^2\theta, \\ D_{12} &= D_{21} = (D_L - D_T)\cos\theta \sin\theta, \\ D_{33} &= D_T, \\ D_{13} &= D_{23} = D_{31} = D_{32} = 0, \end{aligned} \tag{4}$$

with θ given by Eq. (1). In the above, D_L and D_T are, relatively to the fibers, the longitudinal and transverse diffusivities, with $D_L > D_T > 0$.

Having specified the medium, we select the scroll wave to have its axis of rotation (axis of the filament) in the y direction; thus, the y coordinate is not involved in the equations of motion. We are dealing with a spatially two-dimensional problem, in which our goal is to determine the filament's possible drift trajectories in terms of the $\{x,z,t\}$ coordinates. The basic assumption of our approach will be that only the immediate vicinity of the filament is of any relevance in determining its behavior; briefly stated, the filament dynamics is local. (In this paper's conclusion we make some comments on the validity of that approximation.) We focus on the spatial nonuniformity of Eqs. (4), where D_{ij} depends on z through the angle θ: in the vicinity of a typical plane $z = z_0$ ($z_0 = \text{const}$), D_{ij} exhibits a gradient in the z direction.

We now demonstrate that the nonuniformity in the medium can be transformed away, at least in the vicinity of some $z = z_0$, by a transformation of coordinates, which replaces the gradient by a (uniform) convective perturbation, and leads to a standardized formulation of the drift problem. Quantitative and qualitative data for such solutions are available in the literature [9]. The present paper promotes the idea that the case of a uniform convective perturbation can be used as a standard for dealing with the more complex twisted anisotropy.

What is meant here by ''convective perturbation'' can be most succinctly described as follows: In Eq. (2), a small amount of space gradient adds itself to the time differentiation according to

$$\partial_t \rightarrow \partial_t - \mathbf{G} \cdot \boldsymbol{\nabla},$$

where $\mathbf{G}$ is a small constant vector determined by the twist constant k and by the value of z_0. The time derivative in Eq. (3) is not affected because no diffusive term is present.

The main results of our simplifying transformation $\{x,y,z\} \rightarrow \{X,Y,Z\}$ are as follows. First, as indicated above, and as displayed in Eq. (15) further on, it permits us to standardize the drift problem, now restated as follows: To find the drift of a spiral wave in a spatially uniform isotropic medium perturbed by a spatially uniform convection. Second, we obtain and test explicit formulas for the drift trajectories in the actual twisted anisotropic medium.

III. FROM GRADIENT TO SPATIALLY UNIFORM CONVECTION

In outline, the argument involves three successive transformations of the space coordinates. Let the scroll wave's instantaneous axis of rotation have its z coordinate equal to some value z_0 at time t_0. Our assumption of a local dynamics allows us to introduce as our first transformation a linearization of the diffusivity tensor in the vicinity of $z = z_0$; we replace the sinusoidal z dependence of the diffusivity components by a term linear in $z - z_0$. The second transformation rescales the twisted medium globally in such a way that isotropy is restored at $z = z_0$; anisotropy will of course persist or even worsen in other layers of the medium. In particular, the xy components of the diffusivity still show a gradient in the z direction at $z = z_0$. However, because no variables depend on y, we have a two-dimensional spiral drift problem in the xz plane; the problem involves a linear diffusivity gradient, and no convection. Thus, the medium is still nonuniform as well as anisotropic. The third transformation is quadratic in the space coordinates x and z. It is designed to remove the linear diffusivity gradient everywhere, but only to first order in the gradient's amplitude (i.e., to first order in the rate of twist). The transformed medium possesses, instead of a gradient, a convection in the fast variable, and is now fully uniform. A simple mapping becomes available between the standard-drift solution and the one being sought.

Transformation I. Applying the linearization of the D_{ij}, $z \rightarrow \zeta$ according to

$$z = z_0 + \zeta, \quad \theta = \theta_0 + k\zeta \quad (\zeta \text{ small}) \tag{5}$$

yields

$$D_{ij} = D^0_{ij} + 2k(D_L - D_T) D^1_{ij} \zeta + o(\zeta^2), \tag{6}$$

where

$$D^0_{ij} = D_{ij}(\theta \rightarrow \theta_0), \tag{7}$$

$$\begin{aligned} D^1_{11} &= -D^1_{22} = -\cos\theta_0 \sin\theta_0, \\ D^1_{12} &= D^1_{21} = \cos^2\theta_0 - \sin^2\theta_0, \\ D^1_{13} &= D^1_{23} = D^1_{31} = D^1_{32} = D^1_{33} = 0, \end{aligned} \tag{8}$$

and where, from here on, we neglect the term of $o(\zeta^2)$.

We next calculate the diffusion term in Eq. (2). From Eqs. (4) we already have before expansion

$$\begin{aligned} \partial_i D_{ij} \partial_j &= D_{ij} \partial_i \partial_j \\ &= D_{11}\partial_1^2 + D_{22}\partial_2^2 + D_{33}\partial_3^2 + 2D_{12}\partial_1\partial_2. \end{aligned} \tag{9}$$

Since in addition we consider the scroll to be parallel to the y axis, i.e., $\partial_2 u \equiv 0$, we see that only the first and third terms of Eq. (9) contribute to $\partial_i(D_{ij}\partial_j)u$. Finally, with expansion (6), the diffusion term is reduced to

$$\partial_i(D_{ij}\partial_j u) = [(A + B\zeta)\partial_x^2 + D_T\partial_\zeta^2]u, \tag{10}$$

where

$$A = D_L \cos^2\theta_0 + D_T \sin^2\theta_0,$$

$$B = -2k(\cos\theta_0 \sin\theta_0)(D_L - D_T). \tag{11}$$

We conclude from Eq. (10) that, under twisting, the effective two-dimensional diffusivity tensor keeps its diagonal nature; however, its x component acquires a gradient in the z direction. Therefore, in contrast to the case of uniform anisotropy, the medium cannot be made isotropic (even effectively, for the scroll considered) by a trivial rescaling of one of the spatial directions. It can, however, be made spatially uniform, as described further on.

Transformation II. A global rescaling, $(x,\zeta) \to (\xi,\zeta)$:

$$\xi = (D_T/A)^{1/2}x, \tag{12}$$

to obtain local isotropy at $z = z_0$ $(\zeta = 0)$. Equation (10) becomes

$$\partial_i(D_{ij}\partial_j u) = D_T\left[\left(1 + \frac{B}{A}\zeta\right)\partial_\xi^2 + \partial_\zeta^2\right]u, \tag{13}$$

where, at $\zeta = 0$, the operators ∂_ξ^2 and ∂_ζ^2 now have the same coefficient.

Transformation III. A quadratic transformation, $(\xi,\zeta) \to (X,Z)$:

$$X = \xi - \frac{B}{2A}\xi\zeta, \quad Z = \zeta + \frac{B}{4A}\xi^2. \tag{14}$$

For small B/A, and after some partial-derivative algebra, this leads directly to the desired form,

$$\partial_i(D_{ij}\partial_j u) = D_T[\partial_X^2 + \partial_Z^2 + (B/2A)\partial_Z]u + o[(B/A)^2], \tag{15}$$

with A and B given by Eq. (11). The term $(B/2A)\partial_Z u$ corresponds to a convection with velocity $BD_T/2A$ in the $-Z$ direction for the variable u only.

Some comments are of interest at this stage.

(1) The device of a quadratic transformation to remove a gradient was first applied in Ref. [9], where the medium was assumed locally isotropic. The details of the transformation are different, however: In that reference, the transformation is conformal, whereas here, in Eq. (14), it is not.

(2) Comparison of Eqs. (10) and (15) shows that a relative gradient B/A in Eq. (10) gives rise to a convection $B/2A$ in Eq. (15). The factor 1/2, which is not present in Ref. [9], is to be expected here from the fact that the twist, being about the z axis, changes the propagation velocity in the x direction but not in the z direction. In contrast, Ref. [9] deals with a gradient in both principal velocities.

(3) Is transformation (14) the only one, to order B/A, that removes the gradient? Uniqueness (up to trivial translations of order B/A in the XZ plane) can be demonstrated by assuming a general form

$$X = \xi + a_X\xi^2 + b_X\xi\zeta + c_X\zeta^2,$$

$$Z = \zeta + a_Z\xi^2 + b_Z\xi\zeta + c_Z\zeta^2, \tag{16}$$

and requiring the gradient's removal; solving for the coefficients $a_X, \ldots, c_Z$ then yields Eqs. (14).

(4) As expected intuitively from the fact that both gradient and drift are seen in xz projection only, the sign of these quantities does not depend on whether the twist is right or left handed. Indeed, for a given z, changing the sign of k in Eq. (1) also changes the sign of θ (or θ_0), and thus the sign of B in Eq. (11) is invariant. We take $k > 0$ for convenience.

IV. DRIFT VELOCITY AND TRAJECTORY

In this section we make use of the transformations described above in order to predict the actual filament drift in twisted anisotropy on the basis of the (simpler) uniformly convective scenario. Suppose that, in a preliminary calculation or from theory, we have solved, to $o(B/A)$, for the drift velocity of a spiral obeying the FHN equations (2) and (3), but with a diffusivity term given by Eq. (15). We assume, as is in fact the case here, that any drift is entirely gradient induced or convection induced, i.e., that there is no meandering. Because $B/2A$ depends on parameters and coordinates, as shown in Eq. (11), it is convenient to replace that quantity, for reference, by a small and positive, but otherwise arbitrary, standard perturbation G. Thus, we set $BD_T/2A \to G$, and look up the existing solution for the drift velocity $\mathbf{V}$, whose magnitude is proportional to G, and whose direction is independent of G [9]. Hence we are able to refer to a ''standard drift vector'' $\mathbf{V}/G$, independent of G. How is the actual drift of the scroll filament, say $\mathbf{W}$, related to $\mathbf{V}/G$? We consider the instant of time when the centers of the spiral's core and of the scroll's filament coincide with the origin of coordinates $(\zeta = Z = 0)$. Because transformation (14) becomes the identity at that location, we only invert transformation (12) in order to get from $\mathbf{V}/G$ to $\mathbf{W}/(BD_T/2A)$. We then have

$$W_x = \left(\frac{A}{D_T}\right)^{1/2}\left(\frac{BD_T}{2A}\right)\left(\frac{V_X}{G}\right), \tag{17}$$

$$W_z = \left(\frac{BD_T}{2A}\right)\left(\frac{V_Z}{G}\right), \tag{18}$$

the answer to our problem.

In order to determine the equilibrium planes, we examine the sign of V_Z. In what follows it is convenient to select a standard case as typical, and to reverse signs where appropriate. From the study of spiral drift in Ref. [9] it appears that V_Z and B usually have opposite signs, unless the spiral is quite sparse, as happens under weak excitability. Thus, we consider the case of opposite signs and assume $V_Z < 0$, so that $B > 0$, and from Eq. (11)

$$\pi/2k < z < \pi/k \quad (\text{modulo } \pi/k). \tag{19}$$

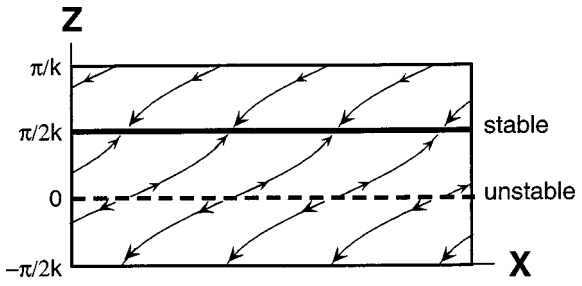

FIG. 2. A family of spatial trajectories for the filament in the case of a clockwise rotating scroll. The filament is oriented along the y direction; its xz projection is a point that moves away from an unstable plane (e.g., dashed line) and towards an adjacent stable plane (e.g., heavy line). Which trajectory is the actual one depends on the filament's initial position.

The complementary intervals have $V_Z>0$. Figure 2 shows the resultant equilibrium planes, stable and unstable.

The complete space-time trajectory of the drifting filament can now be found, still under the assumption of a locally determined drift velocity. We first note that, in the uniform medium XZ, and in the absence of meandering, the drift angle Γ (angle from the $+Z$ direction to $\mathbf{V}$) is constant throughout the (rectilinear) trajectory. How does Γ map into Γ', the local drift angle of the actual filament? From Eqs. (17) and (18) we have

$$\frac{W_z}{W_x}=\left(\frac{D_T}{A}\right)^{1/2}\frac{V_Z}{V_X}, \tag{20}$$

or

$$\cot\Gamma'=\left(\frac{D_T}{A}\right)^{1/2}\cot\Gamma, \tag{21}$$

where Γ is considered known, and $(D_T/A)^{1/2}$ depends on z_0 through Eq. (11). In what follows we drop the subscript ''0'' of Eq. (5) in order to consider the full range of z within the bounds of Eq. (19). To determine the trajectory it is convenient to solve for both x and t in terms of z. Considering $x(z)$ first, we use $dz/dx=W_z/W_x=\cot\Gamma'$, or from the explicit expression for Eq. (21),

$$x=\frac{\tan\Gamma}{k}\int_{\pi/2}^{kz}\left(\frac{D_L}{D_T}\cos^2\theta+\sin^2\theta\right)^{1/2}d\theta \tag{22}$$

(an incomplete elliptic integral of the second kind; the lower integration limit is arbitrary, since we can start the filament at any x). Figure 2 shows a family of such trajectories. In Fig. 3, we compare Eq. (22) with simulation points from Ref. [8].

Next, to find $t(z)$, we combine Eqs. (18) and (11):

$$\frac{dz}{dt}=-\left(\frac{V_Z}{G}\right)\frac{kD_T(D_L-D_T)\cos kz\sin kz}{D_L\cos^2 kz+D_T\sin^2 kz}, \tag{23}$$

which integrates to

$$D_L\ln|\sin kz|-D_T\ln|\cos kz| =-\frac{V_Z}{G}k^2D_T(D_L-D_T)t+\text{const.} \tag{24}$$

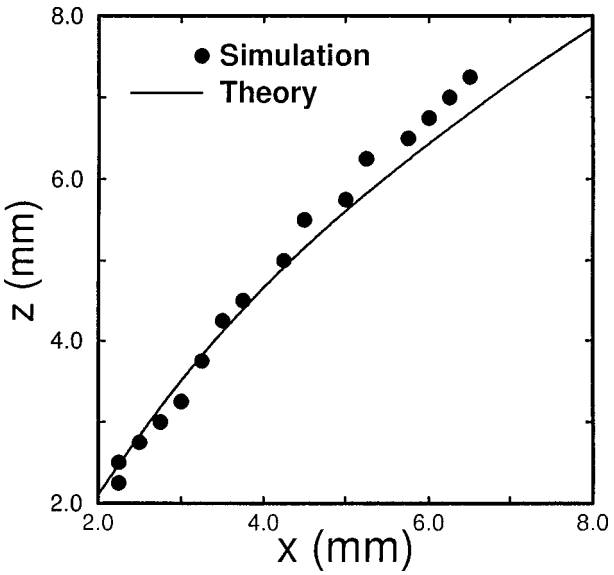

FIG. 3. Trajectory of a simulated filament's xz projection in the FHN-type model. The motion is top right to bottom left, and relates to a clockwise rotating scroll. Formula (22) (solid curve) accounts very well for the drift data (points). The curve, which is a segment from Fig. 2, can be translated arbitrarily in the x direction. In this and the next figure, the z coordinate has been given the origin and scale employed in Ref. [8]. As a consequence, the theoretical stable equilibrium layer, where the filament and fibers are aligned, is at $z=1.875$.

(The origin of t is arbitrary.) This formula is plotted in Fig. 4 together with the corresponding data from Ref. [8]. Close to stable equilibrium ($kz=\pi/2+ks$, $s>0$ small) we have

$$s\approx(\text{const})e^{-t/\tau},\quad \frac{1}{\tau}=-\frac{V_Z}{G}k^2(D_L-D_T), \tag{25}$$

while close to unstable equilibrium ($kz=\pi-ks$, $s>0$ small) we have

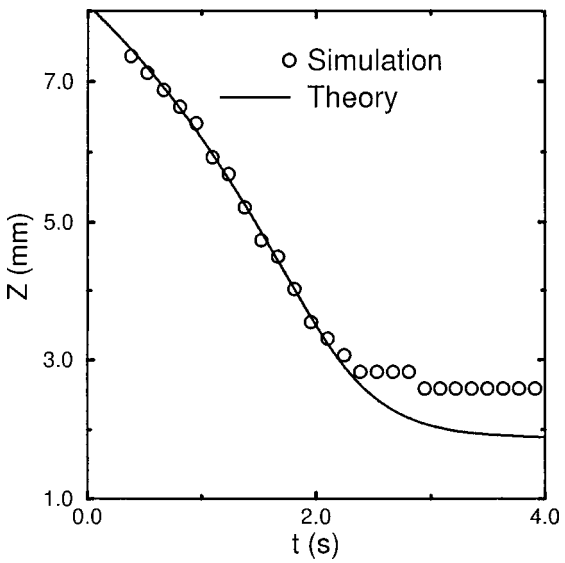

FIG. 4. The filament's z coordinate as a function of time. The origin of t is arbitrary. The agreement between theory and simulation is very good except for some pinning on lattice sites where the perturbation due to the twisted anisotropy is weak.

$$s \approx (\text{const}) e^{+t/\tau'}, \quad \frac{1}{\tau'} = -\frac{V_Z}{G} k^2 \frac{D_T}{D_L}(D_L - D_T). \quad (26)$$

We see that the filament is repelled from the unstable plane at $D_T/D_L \approx 1/9$ times the rate at which it approaches the stable plane.

An interesting alternative exists to the situation just described. Suppose that, in the convective system, simulation or experiment finds $V_Z > 0$, contrary to the $-z$ paradigm studied here. This means a drift opposite to the convection, as happens [9,11] with the sparse spirals (and therefore sparse scrolls) that typically occur in weakly excitable media. In Eqs. (25) and (26) the exponents change sign; the stable and unstable equilibrium planes exchange their nature, and the stable equilibrium layers are now predicted to be those where filament and fibers are mutually at right angles.

V. CONCLUSION

This paper has examined the mathematical relation between two different drift phenomena: (a) the alignment of a scroll filament with the local tissue fibers—or sometimes at right angles to them—due to their twisting orientation, and (b) the drift of a spiral wave in a convective medium. Our central results are the transformed diffusive term of Eq. (15) and the drift formulas (22) and (23). We have here another instance (complementing Refs. [9,10]) where the analytic approach to perturbative vortex drift turns out to be rewarding. The reason is that, while the unperturbed situation is nonlinear and perhaps tractable only numerically, the perturbed one amounts to an essentially linear problem in the perturbation if the latter is not too strong. In the present case, one mode of perturbation can have its effect deduced from that of another mode. More generally, we view our study as a step in an ongoing effort to gain some perturbative understanding of drift phenomena.

Our results carry a specific message about the validity of local filament dynamics, as formulated in our case of a straight filament without torsion. In this case, according to local filament dynamics, the drift of a filament is determined only by its immediate environment. This is our only assumption, which we use to justify a linear expansion of the nonuniform diffusivity components; Figs. 3 and 4 display a high degree of consistency with local filament dynamics. In addition, Fig. 4 is an excellent test for the details of the quadratic-transformation method, Eqs. (14), especially involving the factor $B/2A$ in Eq. (15). Even though we study straight filaments, the message of local dynamics carries over to curved filaments. It confirms the appropriateness of the often-made assumption that the filament's local curvature, if not too strong, determines its local drift, as for example in the shrinking of scroll rings [3]. The relevance to scroll rings is due to the fact that, mathematically, filament curvature amounts to a case of convective perturbation. Universal validity of local filament dynamics should, however, not be inferred from the present work.

As far as the available simulation data are concerned, they are selected from Ref. [8] among those trajectories that are expected to be least affected by proximity to a boundary. That work uses a reasonable adaptation of the FHN model to physiological conditions. The unperturbed scroll ($D_L \to D_T = 1$) then has a cycle wavelength (not too close to the center) of about 25 mm and a pulse width (for the fast variable u) of about 8.5 mm; thus, the scroll is not very dense, at least if only the extent of the fast variable is considered. The total medium thickness is 15 mm, with a total fiber twist of 120°. (Boundary effects appeared to be minor.) On the other hand, we find only about 0.25 mm for the filament diameter (defined by the region where the variable u deviates from its resting value by less than 50% of the maximal amount; the 90% filament is about 1 mm in diameter), a fact which tends to justify our linear expansion. We refer the reader to Ref. [8] for further details about the parameters.

A word of caution is needed concerning sparse scrolls, and the fact that their stable orientation appears to be at right angles to the fibers. Two complications must be kept in mind.

(a) Drift in the $-z$ direction, as we have seen, is related to a model with convection in that direction. Such a model, as we mentioned, is also used to understand the shrinking of scroll rings, and that shrinking is often interpreted in terms of a positive ''tension'' in the filament [12]. Positive tension promotes a form of stability that tends to restore previously straight filaments under perturbation. Conversely, under weak excitability, we expect a negative tension and hence an intrinsic shape instability for a straight filament. We conclude that, under weak excitability, the expected perpendicular alignment process could well be obscured by a competing instability.

(b) A large core, which is typical of sparse spirals, allows the spiral tip to range more widely over z, possibly weakening the convergence of our linear expansion in z.

Finally, we note that, in finite samples of tissue, parallel drift is not the only mechanism that results in the filament's alignment with the fibers. There exists a simultaneous boundary effect, not considered in the present article, which starts at the ends of the filament and eventually helps determine its equilibrium direction [8]. Even though both mechanisms lead to alignment and are concurrent in time, they can be distinguished observationally through their characteristic time scales, which are in general quite different.

ACKNOWLEDGMENTS

We are indebted to J. Jalife for providing our research environment; we thank the American Heart Association, New York State Affiliate, Inc. for financial support (O.B.), and the National Blood and Heart Institute for Grant No. HL39707 (A.M.P. and M.W.).

[1] D. D. Streeter, in *Handbook of Physiology*, edited by R. M. Berne, N. Sperelakis, and S. R. Geigert (Williams and Wilkins, Baltimore, 1979), p. 61 ff.

[2] I. J. LeGrice, B. H. Smaill, L. Z. Chai, S. G. Edgar, J. B. Gavin, and P. J. Hunter, Am. J. Physiol. **269**, H571 (1995).

[3] J. P. Keener and J. J. Tyson, SIAM (Soc. Ind. Appl. Math.)

Rev. **34**, 1 (1992).
[4] A. M. Pertsov and J. Jalife, in *Cardiac Electrophysiology from Cell to Bedside*, edited by D. P. Zipes and J. Jalife (W.B. Saunders, Philadelphia, 1995), Chap. 38, a review.
[5] F. Fenton and A. Karma, Chaos **8**, 20 (1998).
[6] A. V. Panfilov and J. P. Keener, Physica D **84**, 545 (1995).
[7] A. V. Panfilov and J. P. Keener, J. Cardiovasc. Electrophysiol. **4**, 412 (1993).
[8] O. Berenfeld and A. M. Pertsov, J. Theor. Biol. **199**, 383 (1999).
[9] M. Wellner, A. M. Pertsov, and J. Jalife, Phys. Rev. E **59**, 5192 (1999).
[10] M. Wellner, A. M. Pertsov, and J. Jalife, Phys. Rev. E **54**, 1120 (1996).
[11] V. Krinsky, E. Hamm, and V. Voignier, Phys. Rev. Lett. **76**, 3854 (1996).
[12] V. N. Biktashev, A. V. Holden, and H. Zhang, Philos. Trans. R. Soc. London, Ser. A **347**, 611 (1994).